Polymer 91 (2016) 33–40

Contents lists available at ScienceDirect

Polymer

journal homepage: www.elsevier.com/locate/polymer

Water resistant reactive microcapsules for self-healing coatings in harsh environments

Dawei Sun, He Zhang, Xiu-Zhi Tang, Jinglei Yang*

School of Mechanical and Aerospace Engineering, Nanyang Technological University, 639798, Singapore

ARTICLE INFO

Article history:
Received 26 October 2015
Received in revised form
7 March 2016
Accepted 15 March 2016
Available online 17 March 2016

Keywords:
Water resistant microcapsule
Shell tightness
Self-healing anticorrosion coating

ABSTRACT

Double-shelled microcapsules containing liquid 4,4′-bis-methylene cyclohexane diisocyanate (HMDI) with outstanding water resistance are successfully synthesized via combination of interfacial and in-situ polymerization reactions in an oil-in-water emulsion. The diameter and shell thickness of microcapsules increased under lower agitation rate. The relative residue of core content of microcapsules remains more than 90% after 24 days in both ambient open air and water. Manually scratched polymer coatings with both fresh and conditioned microcapsules showed satisfactory anticorrosion performance in salt water via self-healing functionality. In addition, self-healing coatings with fresh microcapsules after immersion in ambient water for 30 days still possessed superior anticorrosion performance.

1. Introduction

Metals and alloys as structural materials are widely applied in the fields of buildings, bridges and pipelines, which are susceptible to be corroded once contact with atmospheric moisture, leading to the failure of function. Polymeric coatings were then largely employed as barriers to retard metal's corrosion. However, protective coatings as the outmost layer are subjective to high risks of damages during the transportation, installation, and service stages, leading to the re-exposure of metal substrates. In order to solve this problem, one novel approach, self-healing function, was introduced within barrier coatings by incorporating microcapsules, which can release healing agents (such as, dicyclopentadiene (DCPD) [1], organic silane [2,3], epoxy [4–6], diisocyanates [7–9], light triggered healing agent [10] and corrosion inhibitors [11,12]) once broken. In this way, damages can be autonomously healed. However, polymeric coatings applied to marine and offshore structures, underground pipelines, and steam conduits need to be continuously exposed in aqueous and/or corrosive environments, which require the embeded capsules to survive therein during service life time. Especially in isocyanates-based microcapsules [8], waterproof property of shell wall is the most noticeable consideration for practical use in one-part self-healing anticorrosion coatings due to the reactivity of isocyanates with water. Recently, modification of shell properties to fulfill practical requirements has attracted increasing interests. Amongst those, altering chemical compositions and structures are widely applied due to their easy operations. Tatiya et al. [13] improved the thermal stability of microcapsules by increasing the degree of cure of shell with dendritic functional monomer as cross-linker. Caruso et al. [14] boosted the mechanical strength of microcapsules by thickening shell walls. Wu et al. [15] prepared solvent-proof microcapsules with superhydrophobic shell. Sun et al. [16] developed hexamethylene diisocyanate (HDI) microcapsules with outstanding resistance to low polar organic solvents via double-layered polyurea capsule shell. Kang et al. [17] covered polymeric microcapsules with a layer of polydopamine to improve thermal and solvents stability. Besides modification of polymeric structures, incorporating inorganic particles into shells was also applied to enhance microcapsules thermal [18,19], mechanical [6,19] and barrier [20,21] properties. For microcapsules containing isocyanates, improvements approaches to organic solvents resistance are currently achieved by multilayer shell structure [16], increasing shell crosslink density [13,15] and hybridization with inorganic particles [22]. Besides organic solvents resistance, the water resistance of encapsulated isocyanates was another unavoidable issue, which can be improved by the Pickering emulsion [23] with nearly 10 wt% loss after 4 days in water and fluorinated aromatic amine functionalized shell [24] maintaining original core contents after 1 day in water. However, long-term water resistance of encapsulated isocyanates is still in a high demand, that microcapsules can survive themselves and perform satisfactorily when formulated in coatings after long-term

* Corresponding author.
E-mail address: mjlyang@ntu.edu.sg (J. Yang).

http://dx.doi.org/10.1016/j.polymer.2016.03.044
0032-3861/

water or moisture's attacks. Although combination of interfacial and in situ polymerization has been reported to encapsulate water inert core materials [25], it is still challenging for the encapsulation of isocyanates which are highly sensitive to urea (necessary in situ polymerization).

Herein, an improved method combining interfacial and in situ polymerization was introduced to encapsulate 4,4′-Methylenebis(cyclohexyl isocyanate) (HMDI), which has lower toxicity and vapor pressure compared with HDI, with double-shelled walls possessing superior resistance to water. Various self-healing coatings containing fresh and conditioned microcapsules displayed satisfactory anticorrosion performances after manual scratches under accelerated corrosion conditions.

2. Experimental

2.1. Materials

4,4′-diphenylmethane diisocyanate (MDI) prepolymer Suprasec 2644 was obtained from Huntsman. HMDI, gum Arabic, tetraethylenepentamine (TEPA), hydrochloric acid solution (HCl, 0.1 M), potassium bromide (KBr), sodium hydroxide (NaOH), and sodium chloride (NaCl) were purchased from Sigma–Aldrich. Epolam 5015 and hardener 5015 used as epoxy coating were supplied by Axson. All chemicals in this study were used as received without further purification.

2.2. Synthesis of double-shelled microcapsules containing HMDI

The microcapsules containing HMDI as core materials were synthesized by combing interfacial and in situ polymerization. Interfacial polymerization was firstly applied to prepare polyurea microcapsules, which are then coated with a layer of PUF shell via in situ polymerization.

2.2.1. Synthesis of polyurea microcapsules

The polyurea microcapsules were prepared via interfacial polymerization in an oil-in-water emulsion system. Firstly, the water phase, 30 ml of deionized (DI) water containing 2.5 wt% of gum Arabic was heated up to 30 °C in a 250 ml beaker, which was placed in a temperature controlled water bath located on a programmable hotplate. Later, the uniform oil phase containing 0.5 g of Suprasec 2644 and 4.5 g of HMDI was emulsified in the surfactant aqueous solution under certain agitation rate (Caframo, model: BDC6015). After the system was stabilized for 45 min at 30 °C, 18.0 g of TEPA aqueous solution (30 wt%) was added to initiate the interfacial polymerization. Meantime, the system temperature was raised to 65 °C. After reaction for 30 min at the designated temperature, the obtained suspension of microcapsule slurry was rinsed with DI water for 3–4 times followed by further coat of PUF shell, as described hereafter.

2.2.2. Formation of PUF shell on polyurea microcapsules

2.00 g urea, 0.50 g ammonium chloride and 0.50 g resorcinol were firstly dissolved in 60 ml DI water in a 250 ml beaker under agitation rate of 200 RPM. Afterwards, the pH value of the solution was adjusted to approximate 3.50 using NaOH and HCl solutions. After stabilization at 55 °C, the system was introduced polyurea microcapsules and 4.5 ml of formaldehyde solution (37 wt%). After reaction for 20 min, the microcapsules suspension was rinsed and washed with DI water for 3 times before air dried for 12 h.

2.3. Characterization of HMDI filled microcapsules

Scanning electron microscope (SEM, JOEL JSM 5600LV) was applied to observe the size, morphology, and shell thickness of the resultant microcapsules. The size distributions of the microcapsules were derived from the statistic of at least 150 individuals using ImageJ in SEM images. Microcapsules were mounted on conductive tape and some of them were ruptured with a razor blade to observe the core–shell structure.

Spectrophotometer (Varian 3100) was applied to obtain FTIR spectras of pure HMDI, Suprasec 2644, capsule core material, pure capsule shell, and shells processed by TEPA solution (10 wt%) mixed with KBr pellet separately in order to identify the composition.

2.4. Thermal property and core fraction of HMDI microcapsules

The thermal property and core fraction of microcapsules were characterized with thermogravimetric analyzer (TGA, Hi-Res Modulated TGA 2950). 10–20 mg of microcapsules were heated in nitrogen atmosphere at a rate of 10 °C/min to 100 °C and then kept isothermal for 10 min to remove residual moisture. Afterwards, the sample temperature was raised to 180 °C followed by 60 min of isothermal to achieve complete evaporation of core material. Finally, the samples were heated to 600 °C for complete decomposition. The core fraction of capsules was derived by consideration of the weight loss of microcapsules and shell at 180 °C.

2.5. Water resistance test

In order to test water resistance, microcapsules were soaked in open air with relative humidity of 60%, water solution with different pH values (pH = 3, 10 wt% NaCl solution and pH = 11 aqueous solution), and tap water with different temperatures (RT, 30 °C and 40 °C), for certain period of time to observe the decrease of relative core fraction (characterized by residual/fresh core fraction). TGA was applied to determine the residual core fraction of treated microcapsules.

2.6. Preparation and characterization of self-healing anticorrosion coatings

Self-healing anticorrosion coatings were prepared by dispersing microcapsules in epoxy resin Epolam 5015. After the removal of the trapped air-bubbles by degasing in a vacuum oven, the mixture was coated onto the treated steel panels and cured at RT for 24 h to form final coating with thickness around 300 μm.

Four types of cured specimens were prepared to compare and evaluate the robustness of microcapsules for anticorrosion performance in aqueous environment. Type I, control coating with pure epoxy resin coated on metal substrate; Type II, self-healing coating containing fresh microcapsules coated on metal substrate; Type III, self-healing coating containing treated microcapsules (immersed in RT water for 24 days) coated on metal substrate; and Type IV, self-healing coating containing fresh microcapsules coated on metal substrate that was immersed in RT water for 30 days.

The anticorrosion tests of the self-healing and control epoxy coatings on steel substrates were carried out by manual scratches with razor blade and then immersion in 10 wt% of NaCl solution (accelerated corrosion condition). After immersion for 24 h, the scratched areas of the specimens were imaged by SEM. Finally, the coatings on steel panel were peeled off after 30 min immersion in acetone under ultrasound conditions to verify the scratches and residual healed materials on the metal surface.

Besides SEM observation, self-healing process was also monitored by EIS experiments (Gamry Reference 600 potentiostat) in electrolyte solutions (1 M sodium chloride solution). The detailed parameters were listed as following, swept frequency: 10^{-2}–10^{5};

and AC amplitude: 20 mV.

3. Results and discussion

3.1. Formation mechanism of double-layered shell

Double-layered capsule shell was formed via combination of interfacial and in-situ polymerizations in the oil/water emulsion system, as illustrated in Fig. 1. Firstly, the mixture of Suprasec 2644 and HMDI was emulsified in the surfactant aqueous solution to generate a stable emulsion system, as schematically shown in Fig. 1a using a single emulsified micro-droplet. After stabilization for 45 min, the inner wall was formed by the reaction between MDI prepolymer along with the introduction of TEPA solutions, as shown in Fig. 1b. With increasing time, the TEPA molecules in the aqueous phase diffused gradually into micro-droplets to thicken the shell, which can inversely retard the diffusion of TEPA until equilibrium [26]. However, the newly formed inner membrane was not rigid enough for easy collection. Therefore, additional PUF layer was deposited on polyurea-microcapsules surface to strengthen the shells for better collectability, as shown in Fig. 1c. In this step, concentrated reaction system and lower oil-water ratio [1] were applied to accelerate the formation and deposition of PUF particles on polyurea microcapsules surface for less consumption of HMDI by urea.

In a typical run of synthesis, the microcapsules were obtained under the agitation rate of 850 RPM. The prepared microcapsules had average diameter of 74.2 ± 14.0 μm and shell thickness of 1.52 ± 0.21 μm.

3.2. Processing optimization of microencapsulation procedure

The influence of agitation rate on microcapsules was investigated and characterized in terms of morphology and core fraction. Subsequently the optimum process was applied for future investigations.

3.2.1. On microcapsules diameter and shell thickness

The size of microcapsules strongly affects self-healing performance [6,27], and it is controllable by adjusting the agitation rate during the emulsification process. As shown in Fig. 2a, the diameter of microcapsules decreases from 100.4 ± 20.3 μm to 18.9 ± 6.3 μm corresponding to the increase in agitation rate from 750 to 1450 RPM, which agrees with previous investigations [1,7]. At higher agitation rate, smaller microcapsules were yielded from smaller oil droplets due to the stronger shear force.

The average shell thickness of final microcapsules as a function of agitation rate was also plotted in Fig. 2a. It is clear that the shell thickness reduced from 1.98 ± 0.45 μm to 0.77 ± 0.17 μm with the increase of agitation rate from 750 to 1450 RPM, which conformed to prior investigation[6]. As demonstrated above, finer oil droplets with larger specific interface area were generated under higher agitation rate. So less TEPA was distributed averagely to every droplet based on constant total amount of TEPA leading to thinner shell [19].

3.2.2. On core contents

Although the size and diameters varied significantly, the core content stabilized relatively at around 70 wt% when the agitation rate was increased from 750 to 1450 RPM, as shown in Fig. 2b. The stable core fraction was mainly due to the outstanding water resistance of shell. Even very thin shell can still prevent the diffusion-in of water molecules efficiently.

The microcapsules prepared under the agitation rate of 850 RPM were chosen as the most representative batch for afterwards property test.

3.3. Morphology

The morphology of the resultant microcapsules was observed with SEM, as presented in Fig. 3. Fig. 3a shows the nearly spherical shaped microcapsules and related size distribution. Microcapsules have course outer surfaces (Fig. 3b) resulted from the deposition of PUF particles [1]. The obvious core–shell structure with rare solid particles adhering to the inner surface is presented in Fig. 3c. The particles are produced from the reaction between the diffused-in water and Suprasec 2644 within droplets [16]. Fig. 3d provides the detailed profile of shell structure, double-layered structure. The shell with whole thickness of 1.5 ± 0.21 μm is mainly composed of inner shell of about 1.3 μm and outer shell of about 0.2 μm. The inner shell is produced from the reaction between TEPA and isocyanates, whereas outer shell is due to the deposition of PUF particles [1]. Final double-layered shells provide enough mechanical stiffness for post processing and act as appropriate barriers to retard the attack of water molecules.

3.4. Determination of microcapsules component

The FTIR spectras of HMDI, core material, Suprasec 2644, shell material and processed shell material were shown in Fig. 4. The

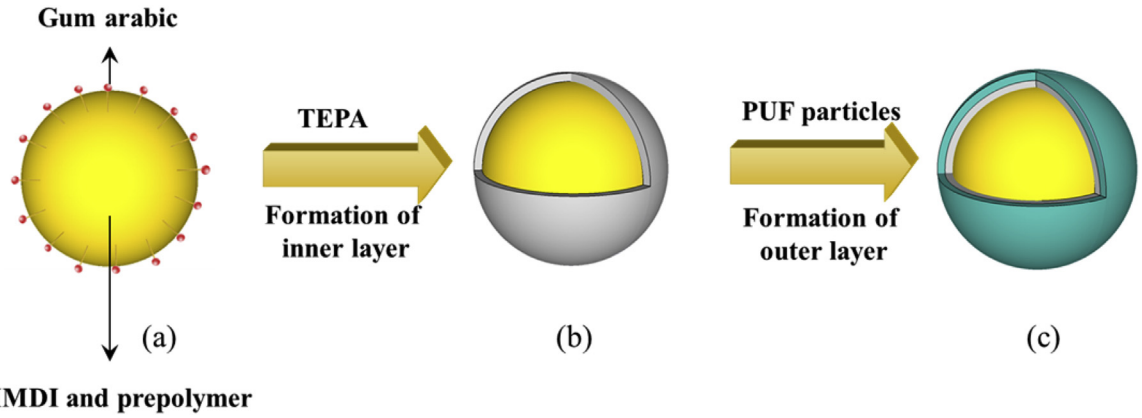

Fig. 1. Schematic formation process of double-layered microcapsule (not to scale): (a) a single oil droplet after emulsification for 45 min; (b) the inner layer of one microcapsule was formed along with the introduction of TEPA solution in emulsion system; and (c) the outer wall of one microcapsule was formed through the deposition of PUF particles.

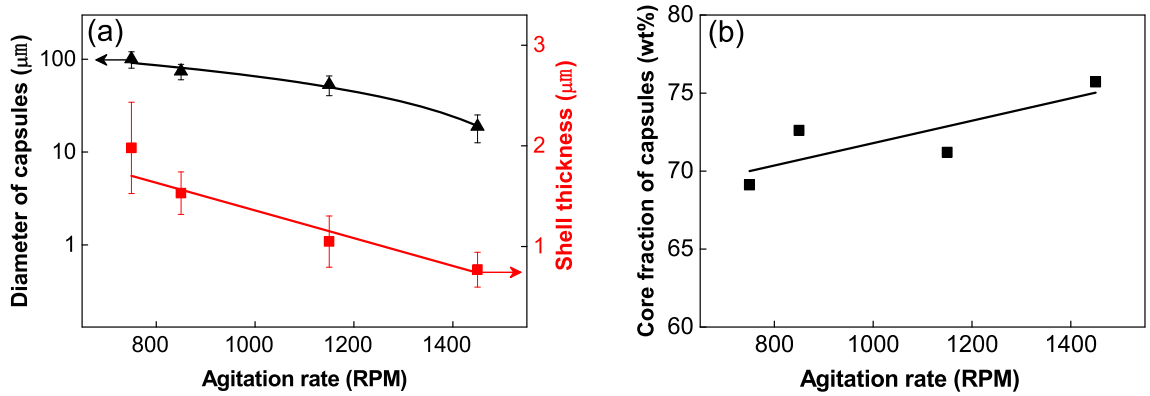

Fig. 2. (a) Diameter (triangle) and shell thickness (square) of microcapsules prepared at different agitation rates; (b) Core fraction of microcapsules prepared at different agitation rates.

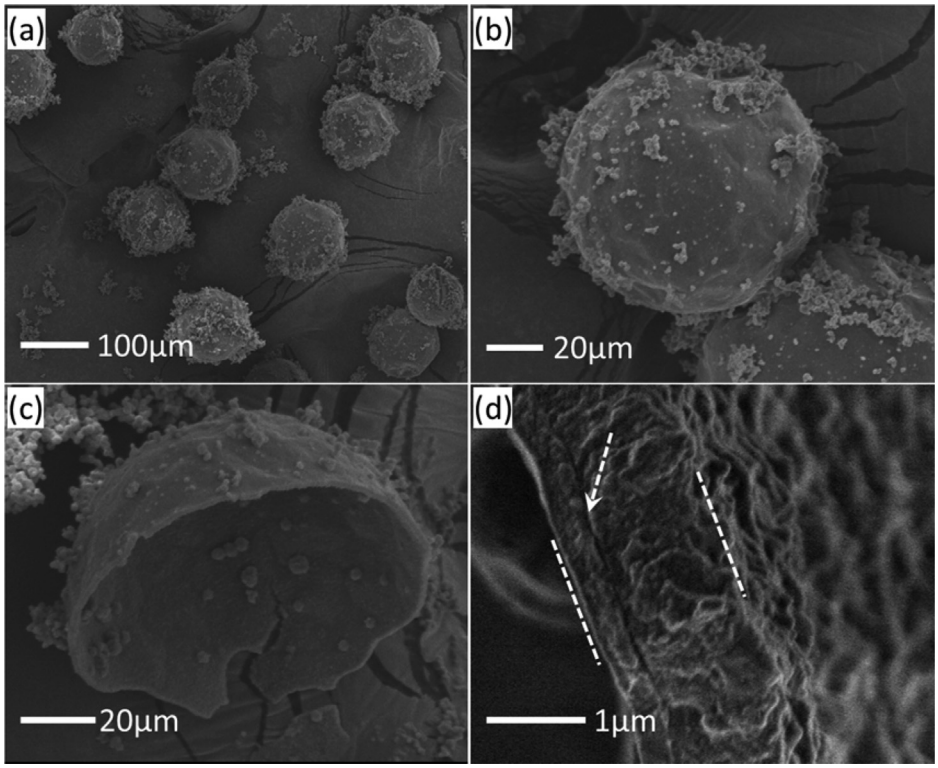

Fig. 3. Morphology of the synthesized microcapsules: (a) overview of spherical shaped microcapsules, (b) enlarged image of individual capsule showing rough outer surface, (c) cross profile of one microcapsule, and (d) double-layered structure of microcapsule's shell.

processed shell material was obtained by storing fresh shell material in TEPA aqueous solution (10 wt%) for 3 days. The nearly identical spectrum curves of HMDI with core material indicated that HMDI was successfully encapsulated with very small amount of Suprasec 2644 because the obscure signal peaks of phenyl group at 1641 cm^{-1} and 1540 cm^{-1} were still detected. Most of Suprasec 2644 within droplets was depleted by diffusion-in water molecules [16]. In the spectrum of fresh shell material, the characteristic signal of NCO stretch at 2269.5 cm^{-1} was detected and disappeared after the treatment by TEPA solution. The existence of NCO within fresh shell is mainly due to the dense shell wall, which isolated shortermly the unreacted NCO groups being consumed. However, the disappearance of this signal peak after shell being processed confirms the reactivity of NCO group.

3.5. Thermal property and core fraction of microcapsules

The weight loss curves of microcapsules, pure HMDI and capsules shell material as a function of temperature are shown in Fig. 5. In the curve, the microcapsules began to lose weight (defined as 5% weight loss) at around 169 °C, and then experienced first major weight loss during the isothermal process at 180 °C, followed by a stable weight plateau until 200 °C. From then on, the microcapsules began the second massive weight loss until 600 °C, leaving slight coke residue. In the curve of shell materials, the beginning weight loss occurred at the isothermal process, and continued degrading massively from 200 °C until 600 °C, leaving coke residue of approximate 10 wt%. The pure HMDI began to lose weight at around 176 °C, and evaporated completely during isothermal

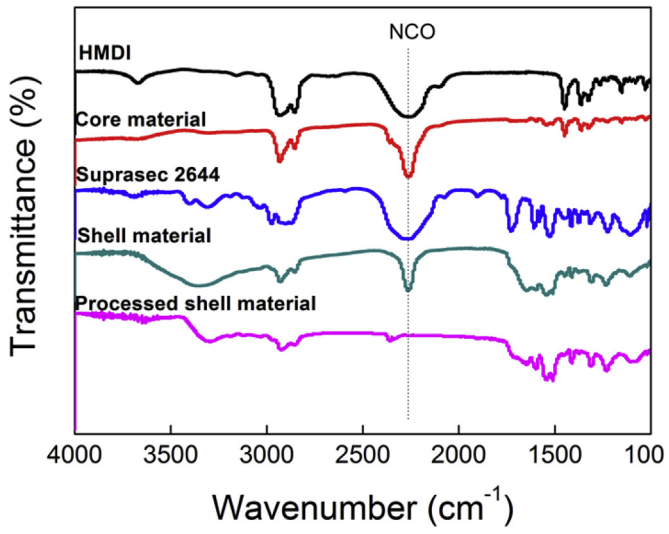

Fig. 4. Comparison of FTIR spectras of capsule's shell and core, Suprasec 2644 and HMDI showing successful encapsulation of HMDI as core material. In addition, the reactive NCO functional groups in capsule's shell disappeared after immersion in TEPA solution (10 wt%).

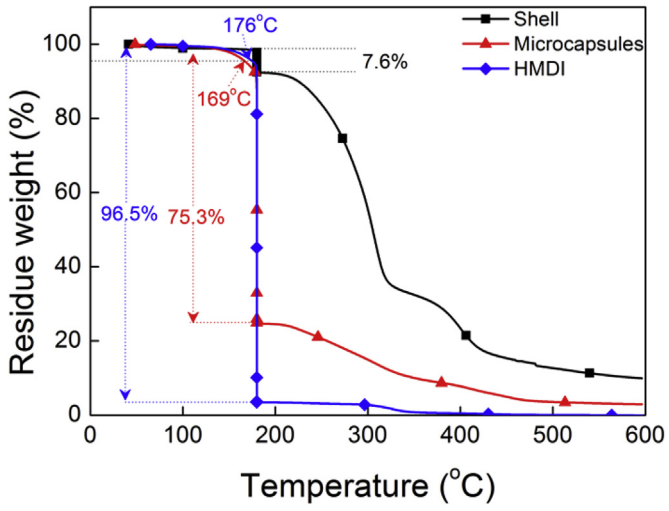

Fig. 5. Thermal performances of resultant microcapsules and constituent materials. TGA curves of the resultant microcapsules, pure HMDI and shell as a function of temperature in N_2 atmosphere. The samples were firstly heated at a rate of 10 °C/min to 100 °C and stabilized for 10 min to remove slight moisture. Then the temperature was raised to 180 °C followed by 60 min of isothermal for complete evaporation of HMDI core. Eventually, the microcapsules were heated to 600 °C for complete vanish.

process at 180 °C. The lower beginning weight loss temperature of microcapsules than pure HMDI is because microcapsules have small shell thickness and the larger specific surface area accelerates the evaporation of liquid core. During the isothermal process, microcapsules release completely core materials resulting in the sequent weight plateau, and the residual shell materials decomposed from 200 °C. The decomposition of shell materials includes two parts: those during isothermal process and major part above 200 °C.

From RT to 180 °C, microcapsules lost weight approximate 75.3 wt% including total liquid core and partial shell materials, while the partial shell materials take 7.6% of fresh shell materials from the related TGA curve. Therefore, the core fraction of microcapsules can be calculated according to following equations:

$$C_{shell} + C_{core} = C_{microcapsules} \quad (1)$$

$$\frac{C_{shell}}{1 - C_{core}} = 7.6\% \quad (2)$$

The weight loss of core, shell and microcapsules by 180 °C were defined as C_{core}, C_{shell} and $C_{microcapsules}$. The typical core fraction of resultant microcapsules prepared under the agitation rate of 850 RPM was 72.3 wt%, which is less than theoretical value due to the existence of PUF particles on the surface of microcapsules.

3.6. Stability of microcapsules in water and aqueous solutions

3.6.1. Resistance to inorganic aqueous solutions

The influence of pH values on the water resistance of microcapsules was tested by immersing fresh microcapsules in solutions from acidity and alkalinity. As illustrated in Fig. 6a, the relative core fraction (residue/original core fraction) decreased gradually with immersion time in all solutions including NaCl solution (10 wt%), acid solution (pH = 3) and alkaline solution (pH = 11). The relative core fraction was 83.1% in NaCl solution (10 wt%), 81% after 24 days in alkali solution (pH = 11) and 78% in acid solution (pH = 3), respectively. Water molecules can diffuse continuously in and consume more HMDI core under longer immersion time. However, the outstanding stability of shell materials at buffered pH value levels protects efficiently encapsulated isocyanates, leaving massive residue after long-standing immersion. The excellent stability in aqueous solutions extends greatly the application environments of final microcapsules.

3.6.2. Pot life

To assess the pot life of synthesized microcapsules, the fresh microcapsules were exposed to ambient open air and immersed in water at different temperatures, respectively. As shown in Fig. 6b, the relative core fraction keeps decreasing with time in humid air, and reached 93.5% residue after 24 days. In addition, the core fraction of microcapsules in water at RT has the similar decrease trend as that in open air, but leaves 91.1% residue after 24 days. The more water molecules diffuse in and consume HMDI core faster than that in open air resulting in less residual of core materials. By comparison with published polyurea [16] or polyurethane [8] microcapsules, it reasonable to believe that the unique shell structure contributes significantly to the outstanding water resistance of final microcapsules.

However, final microcapsules showed compromised resistance to warm water. The HMDI core was completely depleted after 16 days in 30 °C water and 7 days in 40 °C water. The reason for shorter service life in warm water is that higher temperature can accelerate the diffusion of water molecules and increase shell permeability [28].

3.7. Preliminary anticorrosion performance of the formulated self-healing coating

The water resistance of microcapsules influences directly the practical anticorrosion performances of self-healing coatings. Here, anticorrosion tests of four types of coatings are applied to testify the practical water resistance of final microcapsules: (1) control coatings without microcapsules; (2) self-healing coatings containing fresh microcapsules; (3) self-healing coatings containing water treated microcapsules; (4) self-healing coating experiencing water treatment.

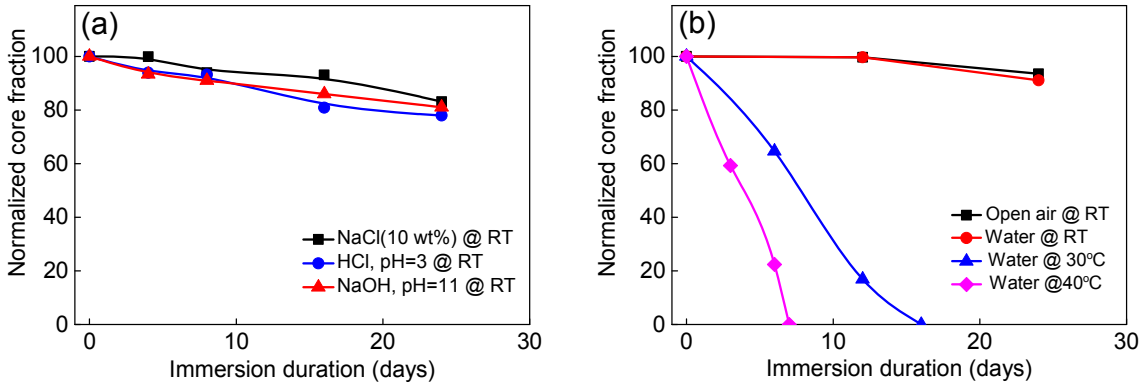

Fig. 6. Stability of the resultant microcapsules synthesized under the agitation rate of 850 RPM. The core fractions of microcapsules decrease with immersion duration in (a) acid solution (pH = 3), alkaline solution (pH = 11) and NaCl solution (10 wt%); (b) open air and water under different atmosphere temperature (RT, 30 °C and 40 °C).

3.7.1. Anticorrosion performance of self-healing coatings containing fresh microcapsules

The fresh microcapsules were dispersed within epoxy resin at a concentration of 10 wt% as self-healing coatings. Besides, control specimens with pure epoxy resin were also prepared for comparison. The anticorrosion tests of specimens were performed under accelerated corrosion conditions, and Fig. 7a and b displayed related experiment results. Obviously, the control specimen experienced severe rust at the scratched area (Fig. 7a_1), while the self-healing specimen was totally free of rust (Fig. 7b_1) after 1 day immersion in salt water (10 wt%). The outstanding anticorrosion function of self-healing coating towards steel substrates was attributed to the fact that the released healing agent from ruptured microcapsules can seal and heal automatically the damaged area after drying, as shown in Fig. 7b_2. However, the empty crack within control specimens (Fig. 7a_2) results in the direct exposure of steel substrates to surrounding corrosive solutions. In addition, the scratches on the surface of specimen substrates (Fig. 7b_3) demonstrated the complete penetration through of coating by manual scratching using blades.

Moreover, the anticorrosion process of self-healing coating containing fresh microcapsules was further characterized with Electrochemical impedance Spectroscopy (EIS) based on published model (Fig. 8a) and equivalent circuit (Fig. 8b) [29]. The swept frequency varied from 10^5 Hz to 10^{-2} Hz, and impedance modulus (Z_{mod}) and phase angel of circuit were obtained as final experiment results. In addition, the healing resistance ($R_{healing}$) obtained from equivalent circuit can supply efficient information about the self-healing process. As shown in Fig. 8c, the Z_{mod} and phase angel of circuit varies dramatically with the swept frequency. Besides, the impedance of scratched area ($R_{healing}$) can be obtained by fitting EIS data to an equivalent circuit (Fig. 8b) through Gamry software. Obviously, the $R_{healing}$ increased from 965 Ω to 5251 Ω when the immersion durations of self-healing samples in NaCl solutions increase from 4h to 24h, as shown in Fig. 8d. The higher $R_{healing}$ under longer immersion time means that more healing agent was released and solidified at the damage area.

3.7.2. Anticorrosion performance of self-healing coatings containing water treated microcapsules

Water treated microcapsules were prepared by immersing fresh microcapsules in tap water for 24 days at RT and then incorporated into epoxy resin for further anticorrosion test. The anticorrosion performances are shown in Fig. 7c and d. It is clear from Fig. 7c_1 that the scratched specimen was not corroded completely after 1 day immersion in salt water. Microscopic observation of scratched areas confirmed the occurrence of self-healing phenomenon as shown in Fig. 7c_2. This verifies enough residue of HMDI core in microcapsules to perform self-healing function after 24 days in water, which is in agreement with the TGA test results in Fig. 6b.

When corrosion duration of specimens in salt water was extended from 1 day to 5 days, the healed self-healing specimens are still able to resist the corrosion of salt water solution (10 wt%) as shown in Fig. 7d_1. This proved that the cured polyurea at the scratched area (Fig. 7d_2) possesses high robustness to isolate outer water molecules. In addition, the self-healing coating was penetrated completely leaving scratches and residual healing agent on the substrates surface (Fig. 7c_3 and Fig. 7d_3).

3.7.3. Anticorrosion performance of self-healing coatings experiencing water treatment

In order to test the practical service life, the self-healing coatings with fresh microcapsules were aged in water for 30 days at RT. The final anticorrosion performance was shown in Fig. 7e. As demonstrated in Fig. 7e_1, treated self-healing coatings still presented superior anticorrosion performance at the damaged area after 1 day immersion in salt water. The sealed scratches (Fig. 7e_2) and residue at substrates surface (Fig. 7e_3) confirmed the occurrence of self-healing and complete penetration of self-healing coating.

4. Conclusion

HMDI microcapsules with superior water resistance were successfully prepared by combing interfacial and in-situ polymerization. The achieved progress was presented as followed:

- The microcapsules size can be adjusted from 100 μm to 18 μm corresponding to the increase of agitation rate from 750 to 1450 RPM, and the shell thickness decreases from 2 μm to 0.7 μm. Meanwhile, the core contents are stabilized relatively at around 70 wt%.
- The final double-shelled wall possesses superior resistance to water. The relative residues of core contents after exposure in both water and open air for 24 days at RT were beyond 90%, and stabilized at around 80% even in acid and alkaline water solutions. However, water resistance was inversed at warmer atmosphere.
- Fresh and those experiencing various water process microcapsules displayed excellent anticorrosion self-healing performance towards steel panels under accelerated corrosion conditions.

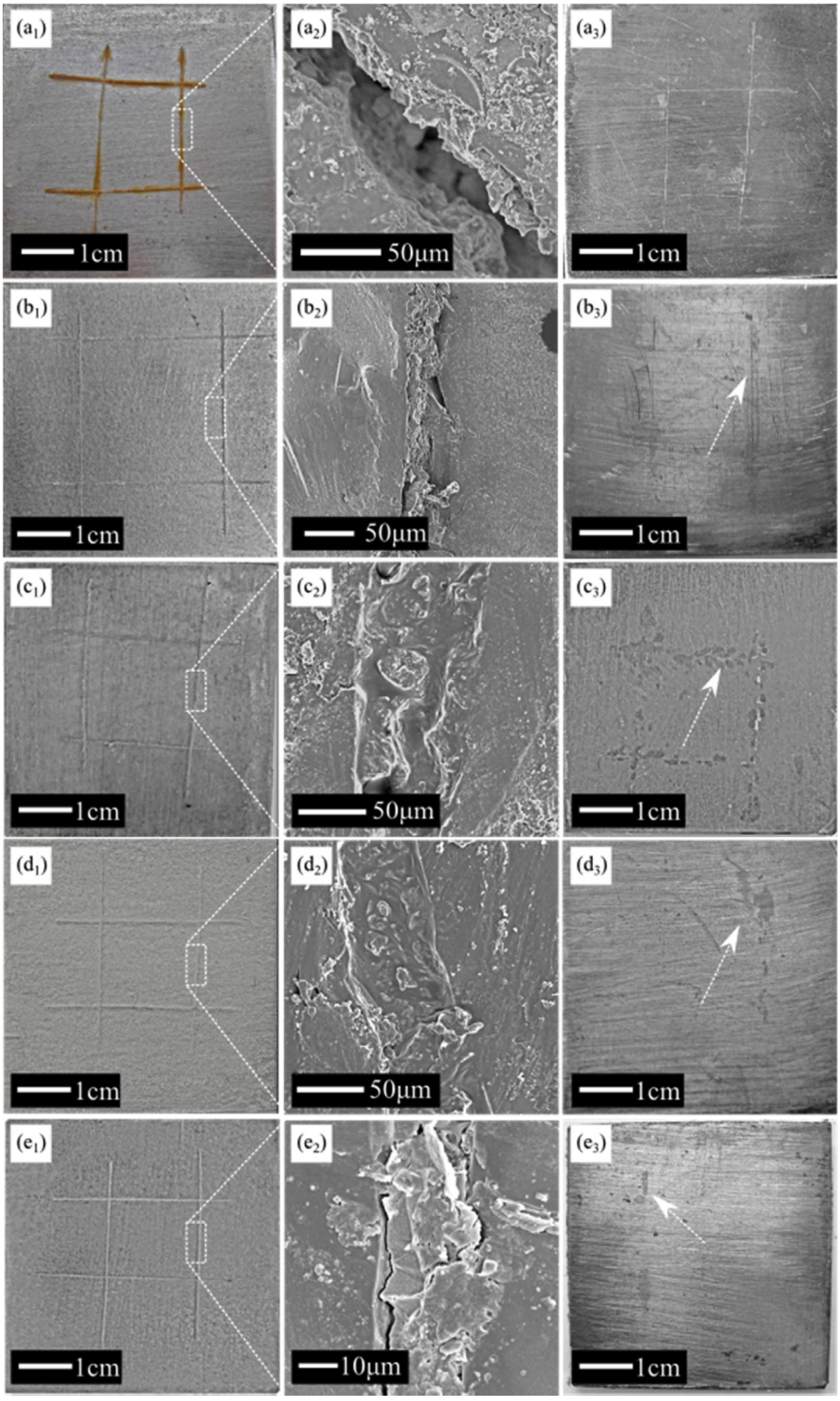

Fig. 7. The corrosion protection of steel panel coated with neat epoxy (a_1) and self-healing coating which is embedded with fresh microcapsules (b_1) experiencing immersion in salt water (10 wt%) for 24 h at RT as regular corrosion test conditions. In addition, microcapsules after immersion in water for 24 days still displayed outstanding self-healing performance in regular corrosion protection experiments (c_1) and extended immersion time (d_1, 5days) in salt water solution (10 wt%). Subsequently, the self-healing specimens without damages were firstly immersed in water for 30 days followed by manual scratches, and then the scratched specimens (e_1) was fully free of rust after regular test conditions. The detailed observations of scratches of respective specimens from SEM were presented in a_2, b_2, c_2, d_2, and e_2. Obviously, the scratches of control samples were empty comparing to other self-healing specimen scratches were sealed completely by materials produced from self-healing process. In addition, the clear scratches or residue from healing agents after removing surface coatings (a_3, b_3, c_3, d_3 and e_3) confirmed the complete penetration through coating after manual scratches.

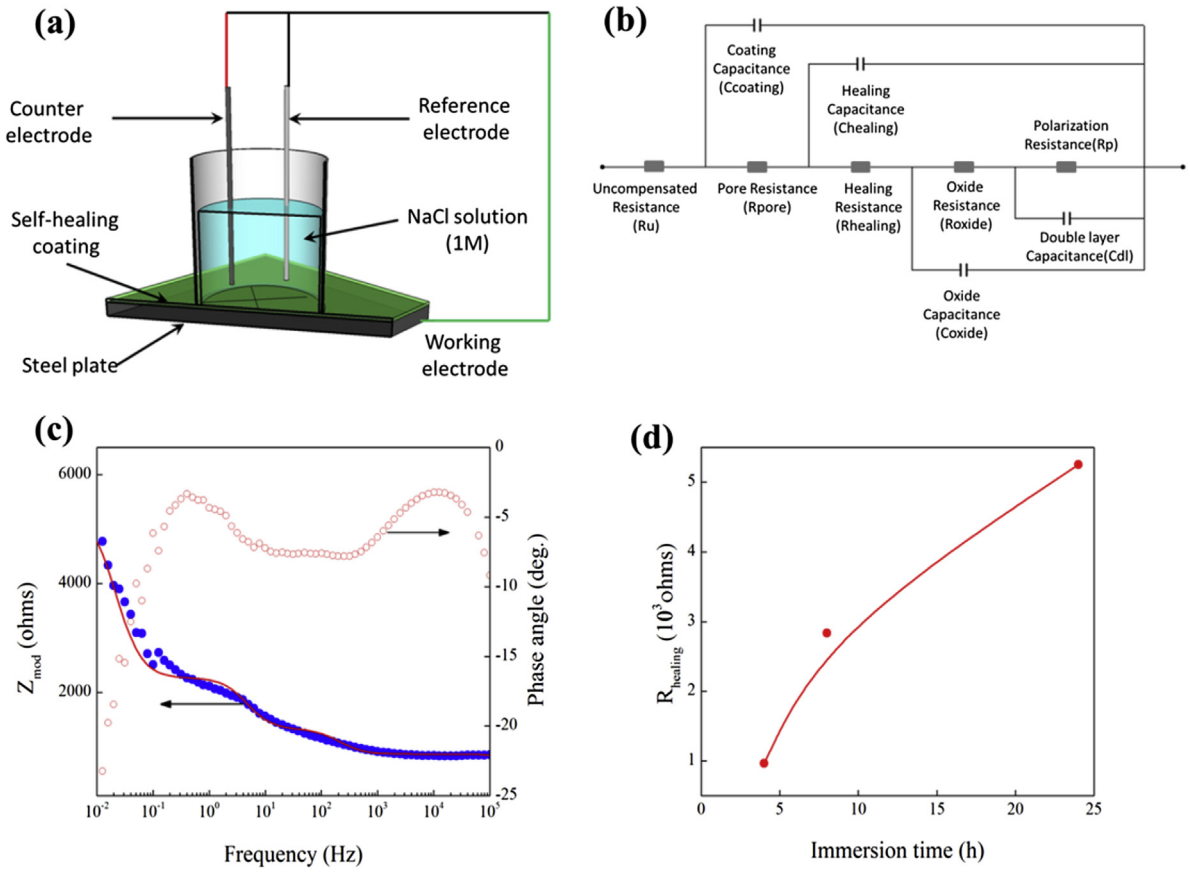

Fig. 8. (a) The schematic picture of EIS experiment model. (b) The equivalent circuit applied to obtain the resistance due to healing ($R_{healing}$) by curve fitting. (c) The electrochemical impedance of scratched self-healing coating (containing fresh microcapsules at a concentration of 10 wt% with final coating thickness around 300–400 μm) characterized with bode plots (impedance module, Z_{mod}, and phase angel) and fitted curves after 4h in 1M salt solution. (d) The healing resistance ($R_{healing}$) of scratched self-healing coating increasing with longer immersion durations in 1M NaCl solution.

In conclusion, the success of water resistant microcapsules provides a promising approach to push one-component, catalyst-free self-healing systems closer to practical applications.

Acknowledgement

The authors appreciate the financial support from the Ministry of Education of Singapore (Grant #: RG15/13).

References

[1] E.N. Brown, M.R. Kessler, N.R. Sottos, S.R. White, J. Microencapsul. 20 (6) (2003) 719–730.
[2] S.H. Cho, H.M. Andersson, S.R. White, N.R. Sottos, P.V. Braun, Adv. Mater 18 (8) (2006) 997–1000.
[3] M. Huang, H. Zhang, J. Yang, Corros. Sci. 65 (2012) 561–566.
[4] L. Yuan, G. Liang, J. Xie, L. Li, J. Guo, Polymer 47 (15) (2006) 5338–5349.
[5] H. Zhang, J. Yang, J. Mater. Chem. A 1 (41) (2013) 12715–12720.
[6] Y.M. Ma, L. Zhang, G.Y. Nie, Study on effects of the nano reinforcing material on the mechanical properties of self-healing composites, in: C.R. Bowen (Ed.), Smart. Mater. Struct, 487, Trans Tech Publications Ltd, Stafa-Zurich, 2014, pp. 20–24.
[7] J.L. Yang, M.W. Keller, J.S. Moore, S.R. White, N.R. Sottos, Macromolecules 41 (24) (2008) 9650–9655.
[8] M. Huang, J. Yang, J. Mater. Chem. 21 (30) (2011) 11123–11130.
[9] W. Wang, L. Xu, X. Li, Y. Yang, E. An, Corros. Sci. 80 (2014) 528–535.
[10] Y.K. Song, C.M. Chung, Polym. Chem. 4 (18) (2013) 4940–4947.
[11] D.G. Shchukin, H. Möhwald, Adv. Funct. Mater 17 (9) (2007) 1451–1458.
[12] M.L. Zheludkevich, D.G. Shchukin, K.A. Yasakau, H. Möhwald, M.G.S. Ferreira, Chem. Mater 19 (3) (2007) 402–411.
[13] P.D. Tatiya, R.K. Hedaoo, P.P. Mahulikar, V.V. Gite, Ind. Eng. Chem. Res. 52 (4) (2013) 1562–1570.
[14] M.M. Caruso, B.J. Blaiszik, H. Jin, S.R. Schelkopf, D.S. Stradley, N.R. Sottos, S.R. White, J.S. Moore, ACS. Appl. Mater. Inter 2 (4) (2010) 1195–1199.
[15] G. Wu, J. An, X.Z. Tang, Y. Xiang, J. Yang, Adv. Funct. Mater 24 (43) (2014) 6751–6761.
[16] D. Sun, J. An, G. Wu, J. Yang, J. Mater. Chem. A 3 (8) (2015) 4435–4444.
[17] S. Kang, M. Baginska, S.R. White, N.R. Sottos, ACS. Appl. Mater. Inter 7 (20) (2015) 10952–10956.
[18] A. Fereidoon, M.G. Ahangari, M. Jahanshahi, J. Polym. Res. 20 (6) (2013) 151.
[19] M. Li, M.R. Chen, Z.S. Wu, Appl. Energ 127 (2014) 166–171.
[20] C.J. Fan, X.D. Zhou, Polym. Advan. Technol. 20 (12) (2009) 934–939.
[21] M.W. Patchan, B.W. Fuller, L.M. Baird, P.K. Gong, E.C. Walter, B.J. Vidmar, I. Kyei, Z. Xia, J.J. Benkoski, ACS. Appl. Mater. Inter 7 (13) (2015) 7315–7323.
[22] G. Wu, J. An, D. Sun, X. Tang, Y. Xiang, J. Yang, J. Mater. Chem. A 2 (30) (2014) 11614–11620.
[23] H. Yi, Y. Yang, X. Gu, J. Huang, C. Wang, J. Mater. Chem. A 3 (26) (2015) 13749–13757.
[24] L.-T.T. Nguyen, X.K.D. Hillewaere, R.F.A. Teixeira, O. van den Berg, F.E. Du Prez, Polym. Chem. 6 (7) (2015) 1159–1170.
[25] G. Li, Y. Feng, P. Gao, X. Li, Polym. Bull. 60 (5) (2008) 725–731.
[26] F.T. MacRitchie, Faraday. Soc. 65 (0) (1969) 2503–2507.
[27] J.D. Rule, N.R. Sottos, S.R. White, Polymer 48 (12) (2007) 3520–3529.
[28] E.C. Suloff, Sorption Behavior of an Aliphatic Series of Aldehydes in the Presence of Poly (Ethylene Terephthalate) Blends Containing Aldehyde Scavenging Agents, Virginia Polytechnic Institute and State University, 2002.
[29] M. Huang, J. Yang, Prog. Org. Coat. 77 (1) (2014) 168–175.